Malaysian Journal of Chemistry, 2024, Vol. 26(3), 169-179
(Special Issue: *The International Conference on Advanced Materials & Sustainable Energy Technologies 2023*)

Synthesis and Characterizations of Titanium Carbide ($Ti_3C_2T_x$) MXene Electrode for Supercapacitors

Jayesh Cherusseri[1,2]* and MA Zaed[1]
[1]Research Centre for Nanomaterials and Energy Technology (RCNMET), School of Engineering and Technology, Sunway University, No. 5 Jalan Universiti, Bandar Sunway, 47500 Selangor Darul Ehsan, Malaysia
[2]School of Engineering and Technology, Sunway University, No. 5 Jalan Universiti, Bandar Sunway, 47500 Selangor Darul Ehsan, Malaysia
*Corresponding author (e-mail: drjayeshpuli@gmail.com)

Transition metal carbides/nitrides and transition metal carbonitrides are collectively known as MXenes. Among the various MXenes available to date, titanium carbide ($Ti_3C_2T_x$) MXene is the most explored material due to its unique characteristics such as large surface area, good electronic conductivity, easy processability, etc. to name a few. Herein, we report the synthesis and characterizations of supercapacitor electrode comprising of $Ti_3C_2T_x$ MXene nanosheets. The $Ti_3C_2T_x$ MXene-based supercapacitor electrode synthesized via slurry coating followed by drop casting procedure. The electrochemical performances of the $Ti_3C_2T_x$ MXene-based supercapacitor electrode are examined in a three-electrode cell set-up using characterization techniques such as electrochemical impedance spectroscopy and cyclic voltammetry. The $Ti_3C_2T_x$ MXene-based supercapacitor electrode delivers a specific capacitance of 108.6 F/g at a scan rate of 5 mV/s. The electrochemical stability of the $Ti_3C_2T_x$ MXene-based supercapacitor is examined for 2000 continuous cycles and exhibits a 100% capacitance retention even after the cycling study.

Keywords: Supercapacitor; MXene; Ti_3AlC_2 MAX; titanium carbide; electrochemical energy storage

Received: March 2024; Accepted: March 2024

The advancements in the area of nanoscience and nanotechnology play a pivotal role in implementing a digital culture to the human era. The developments of novel materials in nanoscale dimensions exhibit extraordinary properties when compared to their bulk counterparts, which enabled them to use in a multitude of applications such as water purification, energy conversion and storage, etc. [1-3]. Modern electronic industry achieved a prominent development in the recent past and play a significant role in boosting the digital technologies for real-time applications. More prominently, development in the consumer electronics such as smart phones, wearable gadgetries, etc. has changed the lifestyle of the community. All these electronic devices require power sources such as batteries to power them [4-5]. The advancement in the rechargeable batteries such as lithium-ion batteries paved a significant role in powering various electronic devices at a cheaper rate [6-8]. The main demerit of rechargeable batteries lies in their low power densities [9-11]. Rechargeable batteries are not suitable for high-power applications such as in electric cars like Tesla. To eradicate this issue, novel electrochemical energy storage devices are evolved, known as electrochemical capacitors or supercapacitors or ultracapacitors [12-13]. The electrochemical capacitor or supercapacitor achieved higher degree of attention due to their faster charge/discharge capabilities, higher power densities and long cycle life [11, 14-15].

The charge storage performance of a super-capacitor depends mainly on the type of electrode-active material used in its electrodes [16-17]. The salient features of a good electrode material for super-capacitor application are large surface area, good electronic conductivity, good chemical stability and good electrochemical stability [18, 19]. The electrode-active materials exhibit different types of charge storage mechanisms. Based on the type of charge storage, supercapacitors are divided in to three categories: (i) electrochemical double layer capacitor (EDLC), (ii) pseudocapacitor (or redox capacitor), and (iii) battery-type hybrid supercapacitor (otherwise known as supercapattery) [20-21]. In an EDLC, the charges are stored by the reversible electrochemical adsorption/desorption of electrolyte-ions in the electrolyte at the electrode/electrolyte interfaces [22-23]. The electrode-active materials are of great importance for EDLC include graphene, carbon nanotubes, carbon aerogel, etc. [24-25]. A pseudo-capacitor stores charges within it by the rapid surface redox reactions. The different types of pseudocapacitive materials explored in the recent past include transition metal dichalcogenides (such as MoS_2, CoS_2, NiS_2, etc.), transition metal oxides (such as V_2O_5, CuO, NiO, Fe_2O_3, etc.), electronically conducting polymers (such as poly-aniline, polypyrrole, etc.), etc. [26-29]. These pseudo-capacitive materials have limitations such as reduced electrical conductivity, higher cost of production, structural instability and restricted cycle life when

†Paper presented at the International Conference on Advanced Materials & Sustainable Energy Technologies 2023

used in supercapacitors [30-31]. These demerits make hurdle for their further exploration in industrial applications. A third category of supercapacitor namely battery-type hybrid supercapacitors are achieved great interest recently. When the battery-type electrodes (means the charge storage phenomenon is mostly by means of diffusion-controlled mechanisms like in batteries) are used in a supercapacitor, it is termed as a supercapattery [32]. An important thing to be noted here is the performance parameter for a supercapattery is specific capacity and not specific capacitance as in the case of EDLC and pseudocapacitor. The performance of EDLC and pseudocapacitor are represented in units of farad per gram (F/g) whereas for supercapattery, it is Coulomb per gram (C/g) or milli-Ampere hour per gram (mAh/g).

The development of highly-efficient electrode-active materials for supercapacitor application at a reduced cost, higher power and energy densities and efficient cyclic stabilities, to satisfy increase in energy demand of the current era of electronic devices is not an option but a necessity [33]. Layered ultrathin two-dimensional (2D) materials are excellent candidates for supercapacitor electrode application due to their large surface area and porous architecture [34]. Transition metal carbides, transition metal nitrides and transition metal carbonitrides are collectively known as MXenes [35]. The various MXenes available are titanium (Ti) carbide ($Ti_3C_2T_x$) MXene [36-37], vanadium carbide MXene [38], Ti nitride MXene [39], chromium carbide MXene [40], etc. Among the various MXenes available to date, $Ti_3C_2T_x$ MXene is the most explored material due to its unique characteristics such as large surface area, good electronic conductivity, easy processability, etc. to name a few [41]. Within this, MXenes possess a general formula $M_{n+1}X_nT_x$ (n = 1, 2, 3 or 4), here 'M' an early transition metal, 'X' is carbon/nitrogen and T_x is a surface terminal group like –O, –OH and/or –F species [42]. MXenes are commonly prepared by selective etching of 'A' element from its parent $M_{n+1}AX_n$ phase, labelled it as MAX, here 'A' corresponds to group IIIA or IVA element in the periodic table [43]. Currently, MXenes are explored with its unique features like higher metallic conductivity, presence of abundant surface functional groups, hydrophilic character, good chemical stability and thermal stability which make it as an efficient electrode material for supercapacitor [44-45]. $Ti_3C_2T_x$ MXene is a largely explored MXene and is widely used as a supercapacitor electrode due to higher Young's modulus, higher melting point, large interlayer spacing and prominent electrical and thermal conductivity [46]. In comparison to other MXenes, $Ti_3C_2T_x$ MXene has prominent interest due to availability of precursor, structural stability and higher electrical conductivity [47].

In this study, we have synthesized $Ti_3C_2T_x$ MXene using fluoride-etching method and further used it as a supercapacitor electrode. The electrochemical performance of the as-synthesized $Ti_3C_2T_x$ MXene is tested in a three-electrode compartment cell using techniques such as electrochemical impedance spectroscopy (EIS) and cyclic voltammetry (CV). 1 M KOH (aqueous) electrolyte is used for the electrochemical testing. The layered 2D $Ti_3C_2T_x$ MXene-based supercapacitor electrode exhibits a specific capacitance of 108.6 F/g at a scan rate of 5 mV/s.

EXPERIMENTAL SECTION

Chemicals and Materials

Perfluorosulfonic acid (PFSA) dispersion and N-methl-2-pyrrolidone (NMP) (C_5H_9NO; 99%) were purchased from Sigma-Aldrich. Super-P carbon black was supplied by Atrish Technic Services Sdn Bhd, Malaysia. Ti powder (99.5%, 325 mesh), aluminum (Al) powder (99.5%, 325 mesh), and graphite powder (99.5%, 325 mesh), LiF and HCl were procured from Alfa Aesar, USA. All reagents were of analytical grade and were used without further purification.

Synthesis of $Ti_3C_2T_x$ MXene

In this study, we combined 15 ml of 9 M HCl solution, 1.6 g LiF, and 5 ml of deionized water. The as-prepared MAX phase is then introduced into this mixture carefully. The mixture was subjected to a controlled heating process at 38°C for 24 h. Heating was performed within a high-density polyethylene container, which was securely sealed with a lid during heating. To ensure thorough and uniform dissolution of the reactants, the mixture was continuously stirred for 24 h. Once this chemical etching reaction was completed, the sample was rinsed repeatedly with deionized water. This rinsing step aimed to neutralize the pH of the sample and effectively remove any excess chemicals. Subsequently, the treated samples were subjected to an overnight drying process in a vacuum oven at 60°C. The resultant material was designated as $Ti_3C_2T_x$ MXene.

Material Characterizations

The microstructure and surface morphology of the samples were examined using scanning electron microscope (SEM) imaging (Hitachi SU8000, Japan). The elemental compositions as well as the distributions of elements in the samples were determined using an energy-dispersive X-ray spectroscope (EDX) connected to the SEM. The mass of samples was measured using a high-precision microbalance (Ohaus, China, Model no EX224) with a readability of 10 µg. The structure and lattice properties of samples were investigated by the D/teX Ultra2 X-ray diffractometer (Rigaku, Japan) with Cu Kα radiation ($\lambda = 0.154$ nm) within a range of $2\theta = 3 - 90°$ at a scan speed of 2°/minute under texture mode.

Preparation of Supercapacitor Electrodes

The $Ti_3C_2T_x$ MXene was used as supercapacitor electrode-active material. Slurry coating was opted to prepare the supercapacitor electrode. In a typical procedure, a slurry was prepared using 3.75 mg active-material (i.e., $Ti_3C_2T_x$ MXene), 0.75 mg Super-P carbon black and 10 µl of PFSA solution. The slurry was mixed thoroughly with the help of agate mortar and pestle by adding NMP drop-wise. This slurry was further drop-casted on to a cleaned nickel (Ni) foam substrate. The as-synthesized supercapacitor electrode was dried at 70ºC in an oven for 12 h thenafter. The geometrical area of the electrode was 1 cm^2. A high-precision microbalance was used to measure the mass of electrode-active material (i.e., $Ti_3C_2T_x$ MXene).

Electrochemical Characterizations

The electrochemical performances of the supercapacitor electrode fabricated using $Ti_3C_2T_x$ MXene are examined using EIS and CV analyses. The supercapacitor electrode was tested in a three-electrode cell configuration by keeping electrode-active material as working electrode, platinum wire as counter electrode, and saturated Calomel electrode as reference electrode [48]. The EIS analysis was carried out within a frequency range of 100000 - 0.01 Hz. The CV analysis was performed within a potential window of 0 - 0.6 V at different scan rates such as 5 mV/s, 10 mV/s, 20 mV/s, 40 mV/s, 60 mV/s, 80 mV/s, and 100 mV/s. All the electrochemical characterizations were carried out using 1 M KOH (aqueous) electrolyte.

RESULTS AND DISCUSSION

The crystal structure of $Ti_3C_2T_x$ MXene is determined using XRD analysis. **Figure 1** shows the XRD spectra of TiC and $Ti_3C_2T_x$ MXene, which display diffraction peaks positioned at $2\theta = 7.2°$ (002), 13.9° (004), 29.2° (012), 36.9° (104), 42.3° (105) and 61.1° (016) and agrees with the crystal structure data for $Ti_3C_2T_x$ reported in the literature [49]. The (002) diffraction peak in Ti_3AlC_2 is found to be broadened and shifted at a lower grazing angle, indicating an increased interlayer spacing of MXene nanosheets caused due to the delamination effect introduced by the etchants; LiF and HCl. The etching treatment using this mixture is not just to etch Al layers in the MAX phase but to delaminate MXene nanosheets simultaneously. Similarly, the secondary phase (004) peak of the Ti_3AlC_2 is also changed towards a lower angle. The XRD analysis confirms the successful formation of $Ti_3C_2T_x$ MXene. The as-synthesized $Ti_3C_2T_x$ MXene exhibited a layered 2D architecture, good chemical and electrochemical stabilities, etc. [50]. These properties are suitable for application as an electrode-active material for supercapacitor application. Hence, we have selected $Ti_3C_2T_x$ MXene as an efficient electrode-active material for supercapacitor application [51]. The microstructure and surface morphology of the $Ti_3C_2T_x$ MXene-based supercapacitor electrode is examined by SEM imaging. **Figure 2(a-c)** represents the SEM images of $Ti_3C_2T_x$ MXene-based supercapacitor electrode at different magnifications. From these images, it is clear that the $Ti_3C_2T_x$ MXene nanosheets are coated on Ni foam substrate via drop-casting method. The three-dimensional morphology of the Ni foam substrate incorporated with layered 2D $Ti_3C_2T_x$ MXene nanosheets boosts the interaction of $Ti_3C_2T_x$ MXene nanosheets with the electrolyte-ions from the electrolyte during the redox reactions. Nanostructured porous architecture is highly preferred for supercapacitor electrode since the electrochemical charge storage of supercapacitor is mainly depends upon the electrode nanostructure [52-53]. The determination of various elements in the $Ti_3C_2T_x$ MXene-based super-capacitor electrode is determined by EDX analysis and **Figure 2(d)** shows the EDX spectrum of the $Ti_3C_2T_x$ MXene-based supercapacitor electrode. The various elements such as nickel (Ni), carbon (C), oxygen (O), Ti, and Al were observed. The presence of Ni arises from the Ni foam substrate used for the fabrication of supercapacitor electrode. The presence of O and Al is inevitable as oxygen arises from the possible air oxidation of the $Ti_3C_2T_x$ MXene nanosheets and Al arises from the unetched reaction product during the synthesis [54]. The distribution of these elements within the $Ti_3C_2T_x$ MXene supercapacitor electrode is determined using EDX elemental mapping and **Figure 3(a-e)** depicts the EDX mapping images for the elements Ni, C, O, Ti, and Al. The elements are uniformly distributed over the entire volume means the uniform distribution of the electrode-active material, $Ti_3C_2T_x$ MXene nanosheets on Ni foam substrate. The synthesis of $Ti_3C_2T_x$ MXene and $Ti_3C_2T_x$ MXene-based supercapacitor electrode is confirmed from the XRD analysis, SEM imaging and EDX mapping analysis.

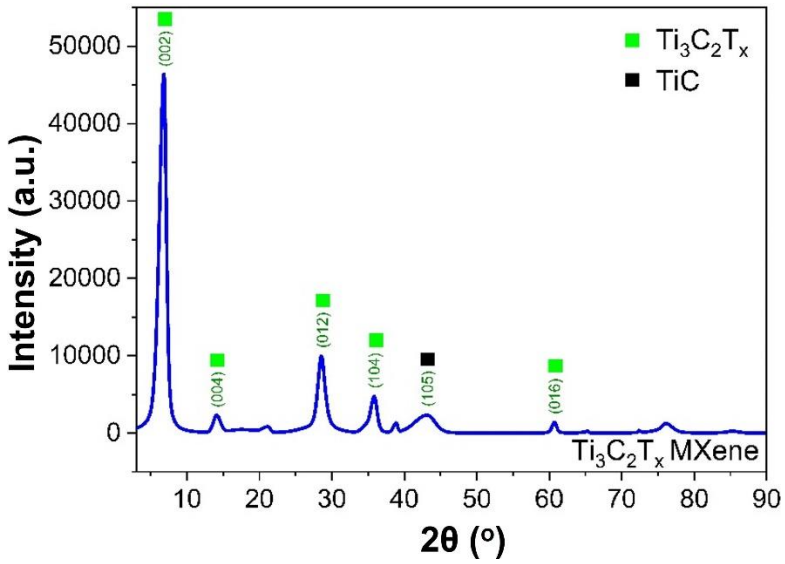

Figure 1. XRD spectra of TiC and $Ti_3C_2T_x$ MXene.

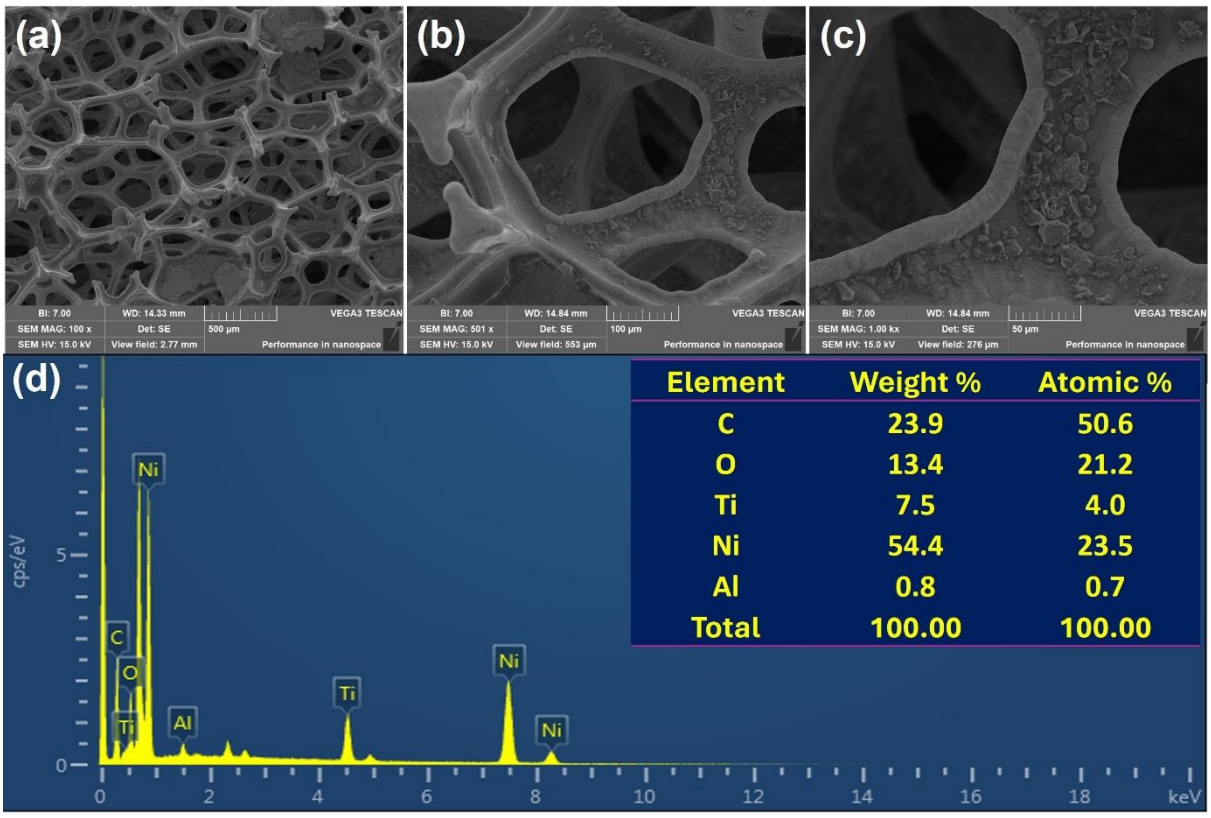

Figure 2. (a-c) SEM images and (d) EDX spectrum of the freshly-prepared supercapacitor electrode comprising of $Ti_3C_2T_x$ MXene coated on Ni foam substrate.

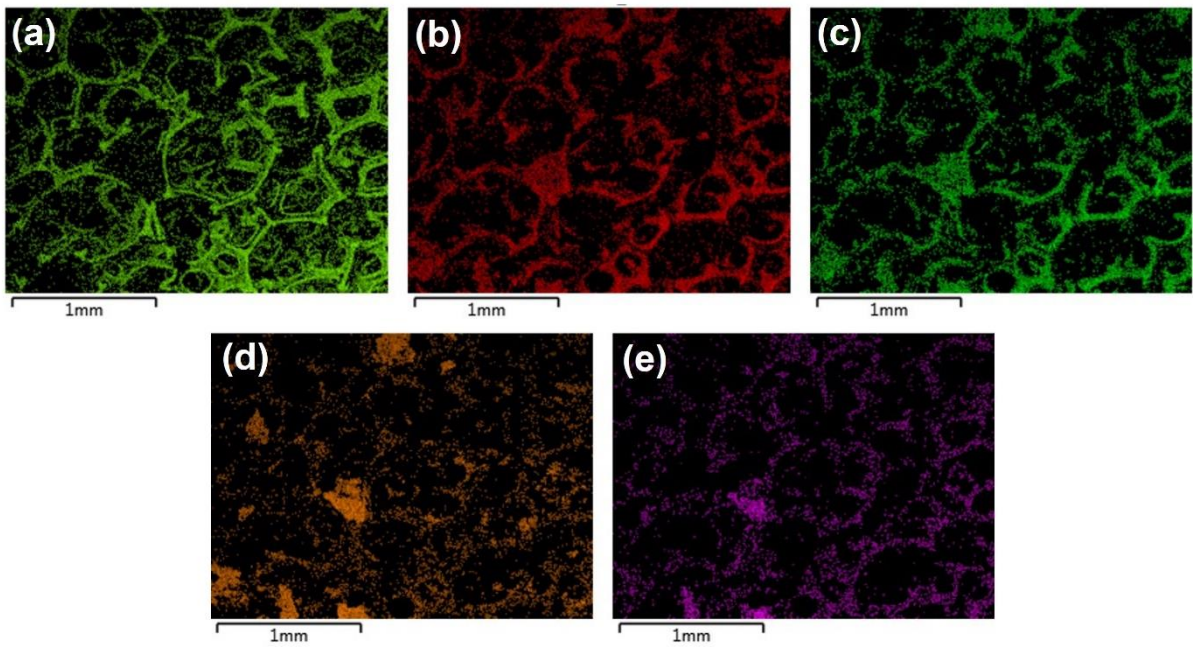

Figure 3. EDX elemental mapping images of the freshly-prepared supercapacitor electrode comprising of $Ti_3C_2T_x$ MXene coated on Ni foam substrate for the elements (a) Ni, (b) C, (c) O, (d) Ti, and (e) Al.

The electrochemical performance of the as-prepared $Ti_3C_2T_x$ MXene-based supercapacitor electrode is evaluated in a three-electrode cell configuration where the $Ti_3C_2T_x$ MXene coated on Ni foam is used as the working electrode, platinum wire used as the counter electrode and saturated Calomel electrode is used as the reference electrode. A freshly-prepared 1 M KOH (aqueous) electrolyte was used for the electrochemical measurements. The capacitive behavior of the $Ti_3C_2T_x$ MXene electrode is evaluated using EIS analysis. **Figure 4(a)** represents the Nyquist plot of $Ti_3C_2T_x$ MXene electrode and **Figure 4(b)** shows the Nyquist plot corresponding to the high-frequency regions. This Nyquist plot exhibits three distinct regions. The first segment is a semi-circle in the high-frequency region and the second one is a Warburg-line with a slope of ~45^o in the mid to high-frequency region [55]. A curve nearly vertical line to Y-axis at low-frequency region can be observed from the Nyquist plot, which represents the ideal capacitive behaviour of the $Ti_3C_2T_x$ MXene. The CV curves of $Ti_3C_2T_x$ MXene electrode is evaluated within a potential range of 0 - 0.6 V and the CV curves obtained at different scan rates is shown in **Figure 5(a)**. These CV curves consist of a pair of oxidation and reduction peaks, indicates pseudocapacitive characteristics of the $Ti_3C_2T_x$ MXene. From these CV curves, it can be observed that there exists a shift in the redox peak position with respect to the scan rate. Since the $Ti_3C_2T_x$ MXene-based supercapacitor electrode exhibits pseudocapacitive behavior, the charge storage is purely by means of redox reactions [56]. Since the redox reactions are purely controlled by the interactions of the electrode-active material with the electrolyte-ions, the scan rate plays a crucial role in determining the rate of reaction to occur. At higher scan rates, due to less residence time, there will be less redox reactions to occur. But at lower scan rates, the probability of getting the electrolyte-ion interaction is high hence there will be profound redox reactions with the electrode-active material. Since the $Ti_3C_2T_x$ MXene exhibits a layered 2D architecture, the electrolyte-ions can move towards the spaces available within the nanosheets [46]. Such porous electrode nanostructures are suitable for attaining high-performance in supercapacitors [57]. The electrochemical performance of $Ti_3C_2T_x$ MXene-based supercapacitor electrode is calculated from the CV analysis and the mass specific capacitance (capacitance per mass of the electrode-active material) is calculated at different scan rates. The mass specific capacitance (F/g) of electrode-active material is calculated from following equation [58],

$$Q_{m,cv} = \frac{1}{M\upsilon V}\int_{V_i}^{V_f} I \times V dV \qquad (1)$$

Where, 'M' is the mass of electrode-active material (only considering the mass of $Ti_3C_2T_x$ MXene), 'I' is the current, 'υ' is the scan rate (in mV/s), 'Δt' is the time and V the potential window. **Figure 5(b)** depicts a comparative analysis of the mass specific capacitance of the $Ti_3C_2T_x$ MXene electrode at different scan rates ranging from 5 mV/s to 100 mV/s. The $Ti_3C_2T_x$ MXene-based supercapacitor electrode delivered a maximum mass specific capacitance of 108.6 F/g at a scan rate of 5 mV/s. As the scan rate increases, the charge storage performance of the $Ti_3C_2T_x$ MXene-based supercapacitor electrode is found to get diminished. The reason is that the electrode-active

material receives enough time (residence time) to interact with the electrolyte-ions within the electrolyte at lower scan rates whereas it is not possible at higher scan rates. To evaluate the cycling stability of the $Ti_3C_2T_x$ MXene-based supercapacitor of electrode, cycling study was carried out using CV analysis for continuous 2000 cycles at a constant scan rate of 50 mV/s. The cycling stability or cycle life is an important performance criterion for commercial application of a supercapacitor since it should be durable for long-run applications [59]. The mass specific capacitance of the $Ti_3C_2T_x$ MXene-based supercapacitor of electrode is found to be unaltered even after completing 2000 cycles. To compare the performance after the cycling study, the CV curves of the $Ti_3C_2T_x$ MXene-based supercapacitor of electrode at its first cycle and 2000th cycle are plotted in **Figure 6**. The area under the CV curve provides an insight on the charge storage capability of supercapacitor electrode. From **Figure 6**, it can be seen that the $Ti_3C_2T_x$ MXene-based supercapacitor electrode after cycling study exhibited an area under the curve same to that of its first cycle without any decrement. The redox peaks are found to have shift due to the activation of supercapacitor electrode, which is very common during cycling due to the opening and closing of new/old pores within the electrode nanostructure [60-62]. This proves the potential of the $Ti_3C_2T_x$ MXene-based supercapacitor electrode for futuristic commercial applications.

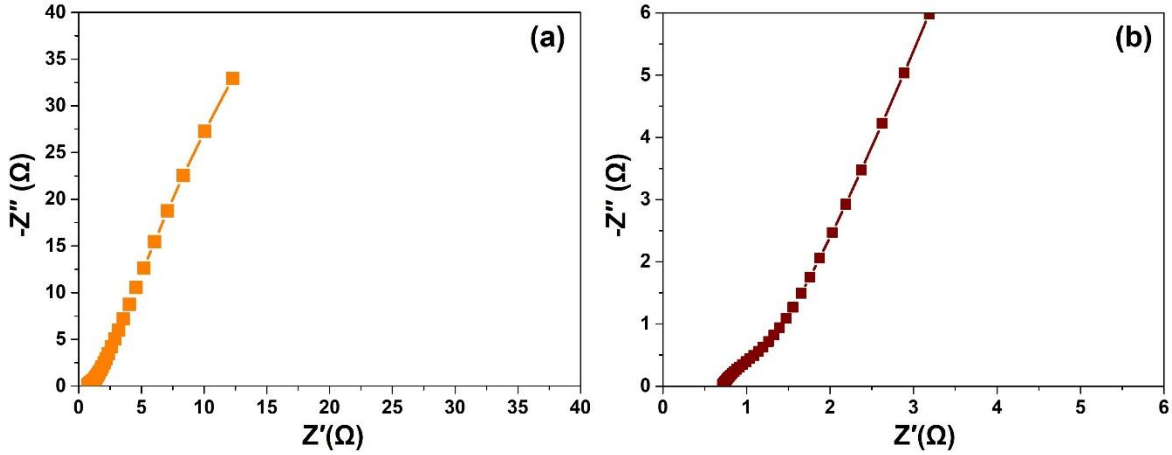

Figure 4. (a) Nyquist plot of $Ti_3C_2T_x$ MXene-based supercapacitor electrode and (b) Nyquist plot of $Ti_3C_2T_x$ MXene-based supercapacitor electrode at high-frequency region.

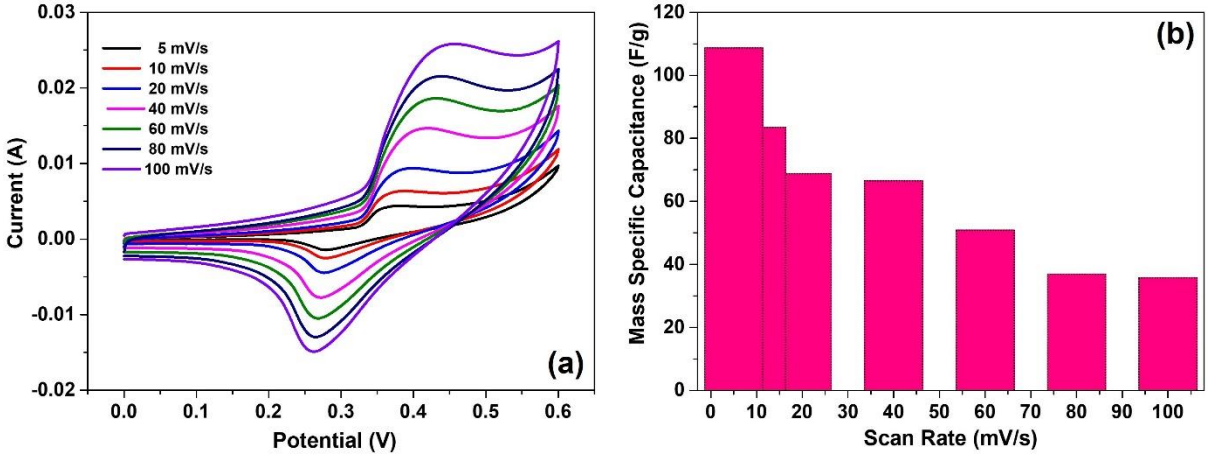

Figure 5. (a) CV curves of $Ti_3C_2T_x$ MXene-based supercapacitor electrode at different scan rates and (b) Plot of variation in the mass specific capacitance of $Ti_3C_2T_x$ MXene-based supercapacitor electrode at different scan rates.

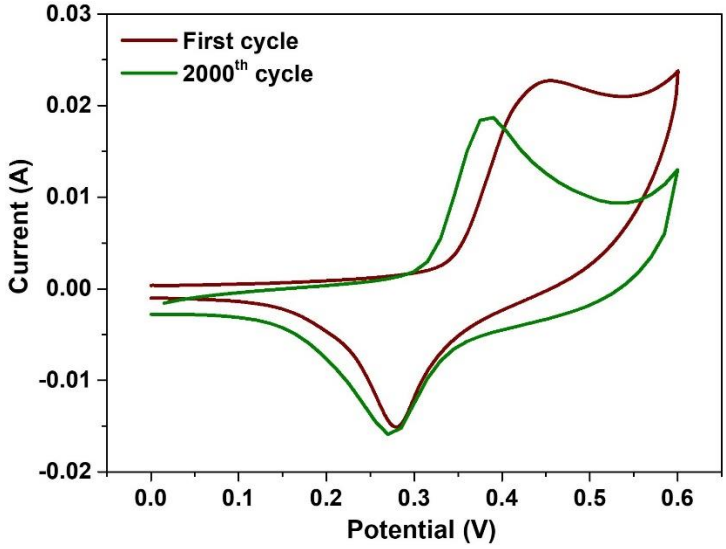

Figure 6. CV curves of $Ti_3C_2T_x$ MXene-based supercapacitor electrode at its first cycle and at 2000th cycle.

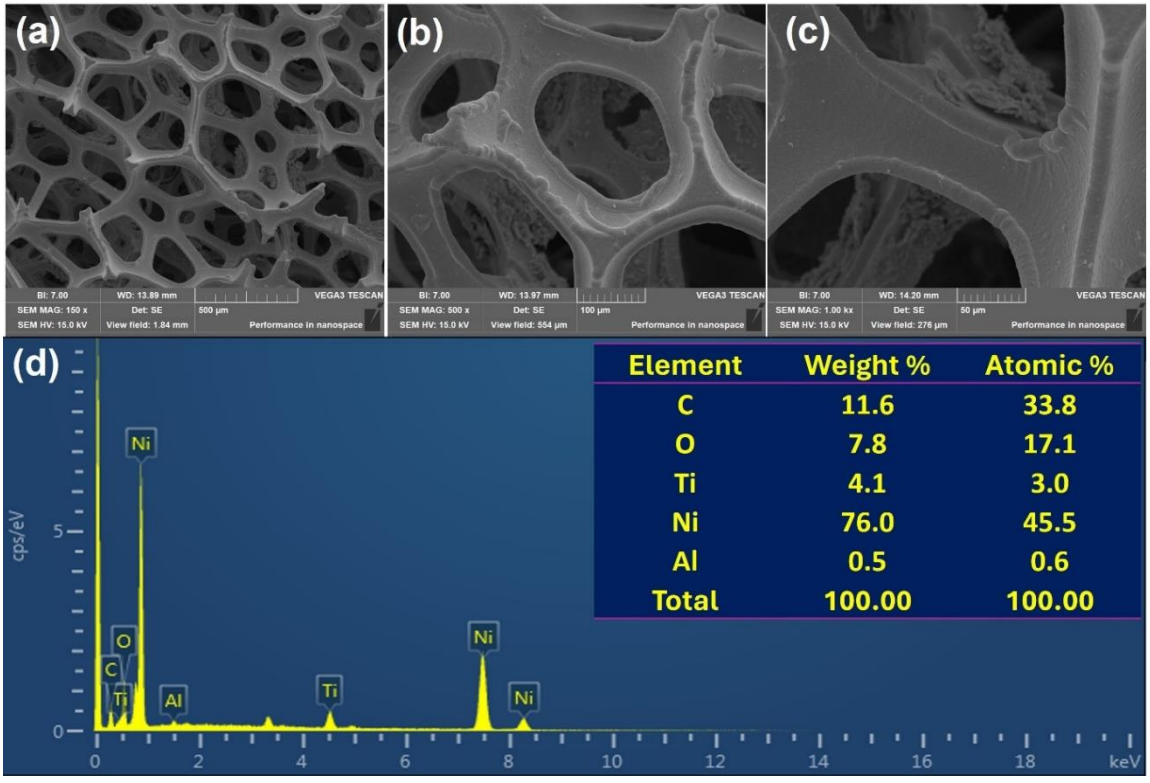

Figure 7. (a-c) SEM images and (d) EDX spectrum of the supercapacitor electrode comprising of $Ti_3C_2T_x$ MXene coated on Ni foam substrate after the completion of 2000 cycles.

The examination of microstructure and surface morphology of the $Ti_3C_2T_x$ MXene-based supercapacitor electrode after the cycling study is mandatory to understand the reason behind 100% capacitance retention even after completing 2000 cycles. **Figure 7(a-c)** represents the SEM images of $Ti_3C_2T_x$ MXene-based supercapacitor electrode after the cycling study. From these SEM images, it is clear that the $Ti_3C_2T_x$ MXene-coated Ni foam substrate is not damaged or not ruptured after the redox reactions during the CV analysis. The portions of the SEM micrographs contain Ni surface with some deposition other than the $Ti_3C_2T_x$ MXene, which are nothing but the accumulated salt from the electrolyte upon drying the electrode after the cycling study (since drying is required for SEM imaging). The charge storage capabilities of the supercapacitor electrode diminishes when the electrode nanostructure ruptures.

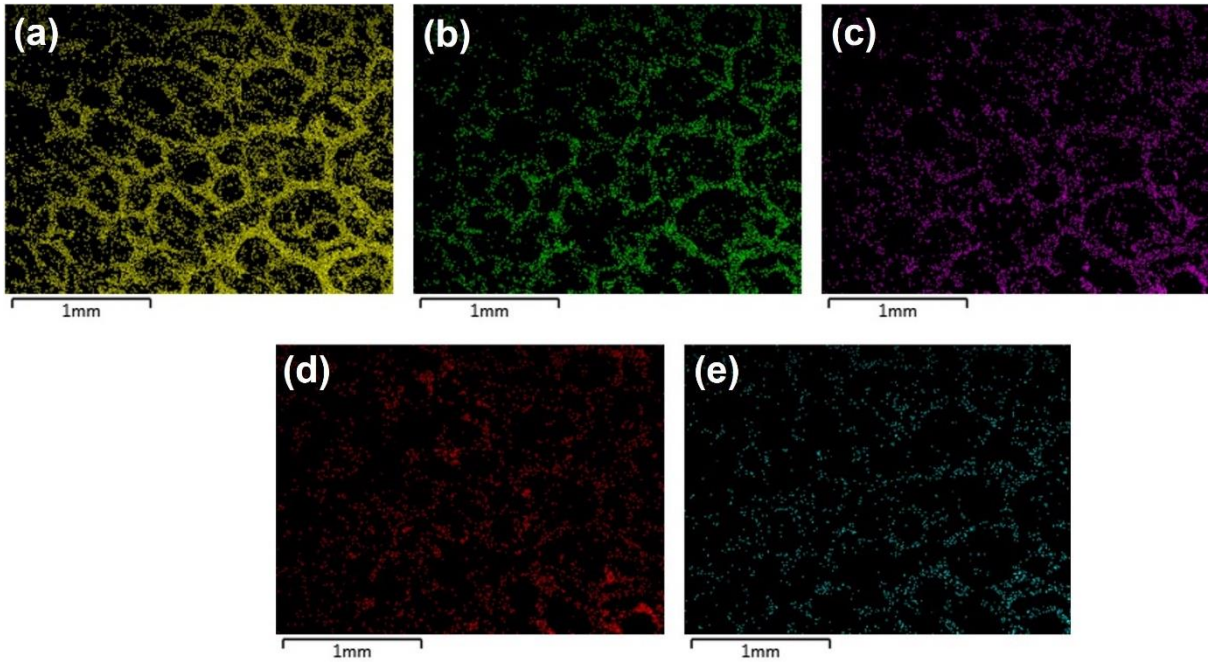

Figure 8. EDX elemental mapping images of the freshly-prepared supercapacitor electrode comprising of $Ti_3C_2T_x$ MXene coated on Ni foam substrate for the elements (a) Ni, (b) O, (c) Ti, (d) C, and (e) Al.

In this study, we have not observed any capacitance deterioration even after the completion of 2000 cycles. The determination of various elements present in the $Ti_3C_2T_x$ MXene-based supercapacitor electrode after the cycling study is carried out by EDX analysis and **Figure 7(d)** shows the EDX spectrum of the supercapacitor electrode. The various elements such as Ni, O, Ti, C, and Al can be observed similar to the freshly-prepared supercapacitor electrode before cycling study. The distribution of these elements within the supercapacitor electrode is determined using EDX elemental mapping. **Figure 8(a-e)** depicts the EDX mapping images for the elements Ni, O, Ti, C, and Al. These elements are uniformly distributed over the entire volume means the presence of electrode-active material, $Ti_3C_2T_x$ MXene on the Ni foam substrate after the cycling study. This shows the excellent stability of the $Ti_3C_2T_x$ MXene-based supercapacitor electrode.

CONCLUSIONS

We have successfully synthesized $Ti_3C_2T_x$ MXene from its respective MAX phase and further used it for fabricating a supercapacitor electrode. The supercapacitor electrode was fabricated by slurry coating method followed by drop-casting technique. The as-prepared $Ti_3C_2T_x$ MXene-based supercapacitor electrode exhibited a porous three-dimensional morphology. The microstructure and surface morphology of the $Ti_3C_2T_x$ MXene-based supercapacitor electrodes were examined using SEM imaging and the distribution of various elements within the supercapacitor electrode were characterized using EDX mapping analysis. The $Ti_3C_2T_x$ MXene-based supercapacitor electrode delivered a maximum mass specific capacitance of 108.6 F/g at a scan rate of 5 mV/s in 1 M KOH (aqueous) electrolyte. The electrochemical cycling stability of $Ti_3C_2T_x$ MXene-based supercapacitor electrode was tested for 2000 continuous cycles by performing CV measurement at a constant scan rate of 50 mV/s and observed that 100% of its initial capacitance was retained even after the cycling study. The reason why the electrode retained its initial capacitance after the cycling study is manifested as the possession of structural integrity and mechanical stability possessed by the $Ti_3C_2T_x$ MXene-based supercapacitor electrode. This was confirmed by examining the microstructure and surface morphology of the $Ti_3C_2T_x$ MXene-based supercapacitor electrode after cycling study using the SEM imaging and EDX analyses. The present study proclaims the preparation of novel hierarchical electrode comprising of $Ti_3C_2T_x$ MXene as an electrode-active material possessing excellent charge storage characteristics for next-generation supercapacitors.

ACKNOWLEDGEMENTS

The authors thank Sunway University Malaysia for providing the necessary facilities to complete this research work.

REFERENCES

1. Krishnan, S. G., Pham, H. D. and Dubal, D. P. (2024) Introduction to supercapacitors, materials and design. In *Supercapacitors*, *Elsevier*, 1–16.

2. Harilal, M. and Krishnan, S. G. (2024) Nanocarbons and electric double-layer capacitors. In *Supercapacitors*, *Elsevier*, 17–43.

3. Thomas, S. A., Vigneshwaran, J., Abinaya, S., Rajendran, D. N., Jose, S. P. and Cherusseri, J. (2024) Water-in-salt electrolyte—toward high-voltage aqueous supercapacitors. In *Supercapacitors*, *Elsevier*, 289–315.

4. Thomas, S. A., Baby, A., Balakrishnan, S. P., Rajendran, D. N. and Cherusseri, J. (2024) Polyoxometalates and redox-active molecular clusters for supercapacitors. In *Supercapacitors*, *Elsevier*, 221–243.

5. Thomas, S. A., Mishra, R. K., Baby, A., Balakrishnan, S. P., Rajendran, D. N. and Cherusseri, J. (2024) Translation of supercapacitor technology from laboratory scale to commercialization. In *Supercapacitors*, *Elsevier*, 371–395.

6. Thomas, S. A. and Cherusseri, J. (2023) A Review of Nb2CT x MXene as an Emerging 2D Material: Synthesis, Applications in Rechargeable Batteries and Supercapacitors, Progress, and Outlook. *Energy & Fuels*, **37**, 7555–7576.

7. Krishnan, S. G., Archana, P., Vidyadharan, B., Misnon, I. I., Vijayan, B. L., Nair, V. M., Gupta, A. and Jose, R. (2016) Modification of capacitive charge storage of TiO2 with nickel doping. *Journal of Alloys and Compounds*, **684**, 328–334.

8. Thomas, S. A. (2023) Layered two-dimensional black phosphorous-based hybrid electrodes for rechargeable batteries. *Journal of Energy Storage*, **73**, 109068.

9. Prasannakumar, A. T., Rohith, R., Cherusseri, J., Mohan, R. R. and Varma, S. J. (2022) High areal capacitance and long cycling stability in asymmetric supercapacitors using binder-free, hierarchical nanostructured Ni3S2/MnO2 hybrid electrodes. *Journal of Energy Storage*, **55**, 105723.

10. Thomas, S. A., Patra, A., Al-Shehri, B. M., Selvaraj, M., Aravind, A. and Rout, C. S. (2022) MXene based hybrid materials for supercapacitors: Recent developments and future perspectives. *Journal of Energy Storage*, **55**, 105765.

11. Thomas, S. A. and Cherusseri, J. (2023) Recent Advances in Synthesis and Properties of Zirconium-Based MXenes for Application in Rechargeable Batteries. *Energy Storage*, **e475**.

12. Thomas, S. A. and Cherusseri, J. (2023) Strategically designing layered two-dimensional SnS2-based hybrid electrodes: A futuristic option for low-cost supercapacitors. *Journal of Energy Chemistry*, **85**, 394–417.

13. Shahid, M., Numan, A., Cherusseri, J., Khalid, M., Somaily, H. and Kaewsaneha, C. (2023) Cobalt hydroxide nanoflakes intercalated into nitrogen-doped reduced graphene oxide's nanosheets for supercapattery application. *Journal of Materials* Research, **38**, 741–752.

14. Baby, A., Sunny, S., Vigneshwaran, J., Abraham, S., P. Jose, S., Saeed, W. S., Pallavolu, M. R., Cherusseri, J. and Puthenveetil Balakrishnan, S. (2023) Azopyridine as a linker molecule in polyaniline-grafted graphene oxide nanocomposite electrodes for asymmetric supercapacitors. *ACS Applied Energy Materials*, **6**, 10442–10456.

15. Thomas, S. A. and Cherusseri, J. (2023) Boron Carbon Nitride (BCN): Emerging Two-Dimensional Nanomaterial for Supercapacitors. *Journal of Materials Chemistry A*, **11**, 23148–23187.

16. Cherusseri, J., Sharma, R. and Kar, K. K. (2015) Nanotechnology advancements on carbon nanotube/polypyrrole composite electrodes for supercapacitors. *Handbook of Polymer Nanocomposites. Processing, Performance and Application: Volume B: Carbon Nanotube Based Polymer Composites*, 479–510.

17. Thomas, S. A., Cherusseri, J. and Khalid, M. A ( ) Comprehensive review on tungsten oxide nanostructures-based electrochromic supercapacitors and machine learning models for design and process parameter optimization. *Energy Storage*, **e499**.

18. Shereef, A., Aleena, P., Kunjumon, J., Jose, A. K., Thomas, S. A., Tomy, M., Xavier, T., Hussain, S. and Sajan, D. (2023) Third order nonlinear optical properties and electrochemical performance of La2CoMnO6 double perovskite. *Materials Science and Engineering: B*, **289**, 116262.

19. Molahalli, V., Chaithrashree, K., Singh, M. K., Agrawal, M., Krishnan, S. G. and Hegde, G. (2023) Past decade of supercapacitor research–Lessons learned for future innovations. *Journal of Energy Storage*, **70**, 108062.

20. Shahid, M., Numan, A., Cherusseri, J., Khalid, M., Somaily, H. and Kaewsaneha, C. (2023) Cobalt hydroxide nanoflakes intercalated into nitrogen-doped reduced graphene oxide's nanosheets for supercapattery application. *Journal of Materials Research*, **38**, 1–12.

21. Cherusseri, J., Pandey, D. and Thomas, J. (2020) Symmetric, asymmetric, and battery-type supercapacitors using two-dimensional nanomaterials and composites. *Batteries & Supercaps*, **3**, 860–875.

22. Izwan Misnon, I., Krishnan, S. G. and Jose, R. (2020) Thin chemisorbed polyaniline film on cobalt oxide as an electrode for hybrid energy storage devices. *ChemistrySelect*, **5**, 7973–7983.

23. Cherusseri, J., Pandey, D., Kumar, K. S., Thomas, J. and Zhai, L. (2020) Flexible supercapacitor electrodes using metal–organic frameworks. *Nanoscale*, **12**, 17649–17662.

24. Kumar, D., Abraham, J. E., Varghese, M., George, J., Balachandran, M. and Cherusseri, J. (2023) Nanocarbon assisted green hydrogen production: Development and recent trends. *International Journal of Hydrogen Energy*.

25. Cherusseri, J. and Kar, K. K. (2015) Recent progress in nanocomposites based on carbon nanomaterials and electronically conducting polymers. *Polymer nanocomposites based on inorganic and organic nanomaterials*, 229–256.

26. Menon, P. S., Thomas, S. A., Anjana, M., Beryl, C., Sajan, D., Vinitha, G. and Philip, R. (2022) The role of defects in the nonlinear optical absorption behavior of pristine and Co-doped V2O5 layered 2D nanostructures. *Journal of Alloys and Compounds*, **907**, 164413.

27. Cherusseri, J. and Kar, K. K. (2016) Ultra-flexible fibrous supercapacitors with carbon nanotube/polypyrrole brush-like electrodes. **4**, 9910–9922.

28. Cherusseri, J., Sambath Kumar, K., Pandey, D., Barrios, E. and Thomas, J. J. S. (2019) Vertically aligned graphene–carbon fiber hybrid electrodes with superlong cycling stability for flexible supercapacitors. **15**, 1902606.

29. Krishnan, S. G., Arulraj, A., Khalid, M., Reddy, M. and Jose, R. (2021) Energy storage in metal cobaltite electrodes: Opportunities & challenges in magnesium cobalt oxide. *Renewable and Sustainable Energy Reviews*, **141**, 110798.

30. Thomas, S. A., Cherusseri, J. and N. Rajendran, D. (2024) 2D Nickel Sulfide Electrodes with Superior Electrochemical Thermal Stability along with Long Cyclic Stability for Supercapatteries. *Energy Technology*, 2301641.

31. Thomas, S. A., Cherusseri, J. and N. Rajendran, D. (2024) Rapid Synthesis of Hierarchical Tin Disulfide (SnS2) Nanostructures by a Microwave-Assisted Hydrothermal Method for High-Performance Supercapatteries. *ACS Applied Electronic Materials*.

32. Krishnan, S. G., Harilal, M., Arshid, N., Jagadish, P., Khalid, M. and Li, L. P. (2021) Rapid microwave-assisted synthesis of MnCo2O4 nanoflakes as a cathode for battery-supercapacitor hybrid. *Journal of Energy Storage*, **44**, 103566.

33. Cherusseri, J., Choudhary, N., Kumar, K. S., Jung, Y. and Thomas, J. (2019) Recent trends in transition metal dichalcogenide based supercapacitor electrodes. *Nanoscale Horizons*, **4**, 840–858.

34. Namsheer, K., Thomas, S., Sharma, A., Thomas, S. A., Raj, K. S., Kumar, V., Gagliardi, A., Aravind, A. and Rout, C. S. (2022) Rational design of selenium inserted 1T/2H mixed-phase molybdenum disulfide for energy storage and pollutant degradation applications. *Nanotechnology*, **33**, 445703.

35. Cherusseri, J. and Kar, K. K. (2016) Polypyrrole-decorated 2D carbon nanosheet electrodes for supercapacitors with high areal capacitance. *RSC advances*, **6**, 60454–60466.

36. Abdah, M. A. A. M., Cherusseri, J., Dzulkarnain, N. A., Mokhtar, M., Su'ait, M. S., Tan, Y. S., Mustafa, M. N., Khalid, M., Numan, A. and Radwan, A. (2023) Facile synthesis of microwave-etched Ti3C2 MXene/activated carbon hybrid for lithium-ion battery anode. *Journal of Electroanalytical Chemistry*, **928**, 117050.

37. Sadanandan, A., Thomas, S. A., Khan, M. E., Alomar, M. S., Pallavolu, M. R. and Cherusseri, J. (2023) A critical review on two-dimensional Ti3C2Tx MXenes for anti-corrosion coatings. *Progress in Organic Coatings*, **183**, 107757.

38. Vahid Mohammadi, A., Hadjikhani, A., Shahbaz-mohamadi, S. and Beidaghi, M. (2017) Two-dimensional vanadium carbide (MXene) as a high-capacity cathode material for rechargeable aluminum batteries. *ACS nano*, **11**, 11135–11144.

39. Urbankowski, P., Anasori, B., Makaryan, T., Er, D., Kota, S., Walsh, P. L., Zhao, M., Shenoy, V. B., Barsoum, M. W. and Gogotsi, Y. (2016) Synthesis of two-dimensional titanium nitride Ti 4 N 3 (MXene). *Nanoscale*, **8**, 11385–11391.

40. Soundiraraju, B., Raghavan, R. and George, B. K. (2020) Chromium carbide nanosheets prepared by selective etching of aluminum from Cr2AlC for hydrazine detection. *ACS Applied Nano Materials*, **3**, 11007–11016.

41. Er, D., Li, J., Naguib, M., Gogotsi, Y. and Shenoy, V. B. (2014) Ti3C2 MXene as a high capacity electrode material for metal (Li, Na, K, Ca) ion batteries. *ACS applied materials & interfaces*, **6**, 11173-11179.

42. Zhong, Q., Li, Y. and Zhang, G. (2021) Two-dimensional MXene-based and MXene-derived photocatalysts: Recent developments and perspectives. *Chemical Engineering Journal*, **409**, 128099.

43. Sokol, M., Natu, V., Kota, S. and Barsoum, M. W. (2019) On the chemical diversity of the MAX phases. *Trends in Chemistry*, **1**, 210–223.

44. Cipolla, L., Somers, M. A. and Hald, J. (2010) Conversion of MX Nitrides to Modified Z-Phase in 9-12% Cr ferritic steels. *Technical University of Denmark*.

45. Richard, B., Thomas, S. A., Reddy M. A., Pallavolu, M. R. and Cherusseri, J. (2023) Minireview on Fluid Manipulation Techniques for the Synthesis and Energy Applications of Two-Dimensional MXenes: Advances, Challenges, and Perspectives. *Energy & Fuels*, **37**, 6999–7013.

46. Wen, Y., Rufford, T. E., Chen, X., Li, N., Lyu, M., Dai, L. and Wang, L. (2017) Nitrogen-doped Ti3C2Tx MXene electrodes for high-performance supercapacitors. *Nano energy*, **38,** 368–376.

47. Zhang, J., Jiang, D., Liao, L., Cui, L., Zheng, R. and Liu, J. (2022) Ti3C2Tx MXene based hybrid electrodes for wearable supercapacitors with varied deformation capabilities. *Chemical Engineering Journal*, **429**, 132232.

48. Vivek, E., Arulraj, A., Krishnan, S. G., Khalid, M. and I, V. P. (2021) Novel nanostructured Nd (OH) 3/g-C3N4 nanocomposites (nanorolls anchored on nanosheets) as reliable electrode material for supercapacitors. *Energy & Fuels*, **35**, 15205–15212.

49. Chen, L., Shi, X., Yu, N., Zhang, X., Du, X. and Lin, J. (2018) Measurement and analysis of thermal conductivity of Ti3C2Tx MXene films. *Materials*, **11**, 1701.

50. Li, L., Wen, J. and Zhang, X. (2020) Progress of Two-Dimensional Ti3C2Tx in Supercapacitors. *ChemSusChem*, **13**, 1296–1329.

51. Kewate, O. J. and Punniyakoti, S. (2023) Ti3A lC2 MAX phase and Ti3C2TX MXene-based composites towards supercapacitor applications: A comprehensive review of synthesis, recent progress, and challenges. *Journal of Energy Storage*, **72**, 108501.

52. Cherusseri, J., Sharma, R. and Kar, K. K. (2016) Helically coiled carbon nanotube electrodes for flexible supercapacitors. *Carbon*, **105**, 113–125.

53. Cherusseri, J., Kumar, K. S., Choudhary, N., Nagaiah, N., Jung, Y., Roy, T. and Thomas, J. (2019) Novel mesoporous electrode materials for symmetric, asymmetric and hybrid supercapacitors. *Nanotechnology*, **30**, 202001.

54. Tian, Y., Ju, M., Luo, Y., Bin, X., Lou, X. and Que, W. (2022) In situ oxygen doped Ti3C2Tx MXene flexible film as supercapacitor electrode. *Chemical Engineering Journal*, **446**, 137451.

55. Zamiri, G., Haseeb, A. M. A., Jagadish, P., Khalid, M., Kong, I. and Krishnan, S. G. (2022) Three-Dimensional Graphene–TiO2–SnO2 Ternary Nanocomposites for High-Performance Asymmetric Supercapacitors. *ACS omega*, **7**, 43981–43991.

56. Huang, H., Su, H., Zhang, H., Xu, L., Chu, X., Hu, C., Liu, H., Chen, N., Liu, F. and Deng, W. (2018) Extraordinary areal and volumetric performance of flexible solid-state micro-supercapacitors based on highly conductive freestanding Ti3C2Tx Films. *Advanced Electronic Materials*, **4**, 1800179.

57. Kunwar, R., Krishnan, S. G., Misnon, I. I., Zabihi, F., Yang, S., Yang, C. -C. and Jose, R. (2021) Transformation of supercapacitive charge storage behaviour in a multi elemental spinel CuMn2O4 nanofibers with alkaline and neutral electrolytes. *Advanced Fiber Materials*, **3**, 265–274.

58. Cherusseri, J. and Kar, K. K. (2016) Hierarchical carbon nanopetal/polypyrrole nanocomposite electrodes with brush-like architecture for supercapacitors. *Physical Chemistry Chemical Physics*, **18**, 8587–8597.

59. Krishnan, S. G., Pham, H. D., Padwal, C., Weerathunga, H., Wang, X., Mahale, K. and Dubal, D. (2023) A stable aqueous ammonium ion hybrid supercapacitor based on pre-intercalated MnOx electrodes and ammonium sulphate electrolyte. *Journal of Power Sources*, **570**, 232994.

60. Cherusseri, J. and Kar, K. K. (2016) Ultra-flexible fibrous supercapacitors with carbon nanotube/ polypyrrole brush-like electrodes. *Journal of Materials Chemistry A*, **4**, 9910–9922.

61. Cherusseri, J. and Kar, K. K. (2015) Hierarchically mesoporous carbon nanopetal based electrodes for flexible supercapacitors with super-long cyclic stability. *Journal of Materials Chemistry A*, **3**, 21586–21598.

62. Krishnan, S. G., Arunachalam, A. and Jagadish, P. (2021) Applications of supercapattery. In *Advances in Supercapacitor and Supercapattery*, *Elsevier*, 311–348.